International Journal of Architectural, Civil and Construction Sciences
ISSN: 2415-1734
Vol:11, No:11, 2017

Experimental Investigation on Residual Stresses in Welded Medium-Walled I-shaped Sections Fabricated from Q460GJ Structural Steel Plates

Qian Zhu, Shidong Nie, Bo Yang, Gang Xiong, Guoxin Dai

***Abstract*—**GJ steel is a new type of high-performance structural steel which has been increasingly adopted in practical engineering. Q460GJ structural steel has a nominal yield strength of 460 MPa, which does not decrease significantly with the increase of steel plate thickness like normal structural steel. Thus, Q460GJ structural steel is normally used in medium-walled welded sections. However, research works on the residual stress in GJ steel members are few though it is one of the vital factors that can affect the member and structural behavior. This article aims to investigate the residual stresses in welded I-shaped sections fabricated from Q460GJ structural steel plates by experimental tests. A total of four full scale welded medium-walled I-shaped sections were tested by sectioning method. Both circular curve correction method and straightening measurement method were adopted in this study to obtain the final magnitude and distribution of the longitudinal residual stresses. In addition, this paper also explores the interaction between flanges and webs. And based on the statistical evaluation of the experimental data, a multilayer residual stress model is proposed.

***Keywords*—**Q460GJ structural steel, residual stresses, sectioning method, Welded medium-walled I-shaped sections.

I. Introduction

IN China, a new type of high performance steel (HPS), named by Q460GJ structural steel was developed. Q460GJ structural steel is increasingly adopted in well-known large scale steel structures [1], like National Olympic Stadium (Birds Nest), Canton Tower. Q460GJ structural steel not only have the advantages of light weight, good plasticity and toughness, but also have good weldability, low thickness effect on yield strength and low yield ratio. Fig. 1 indicates the low thickness effect on nominal yield strengths of Q460GJ, which were compared with the S460 structural steel. From the figure, it can be found that when the steel plate thickness is in the range of 25 mm to 42 mm, the nominal yield strength of Q460GJ structural steel is 5% higher than S460 structural steel. Thus, the favorable performance of Q460GJ structural steel stimulated a great interest in wide usage in building and bridge constructions.

The existence of residual stress which was caused by the manufacturing processes, such as flame-cutting, hot-rolling and welding has a tendency to decrease the strength in stability. Besides, the residual stress is difficult to be predicted by theoretical analyses. Therefore, the distribution and magnitude of residual stresses is obtained by experimental method.

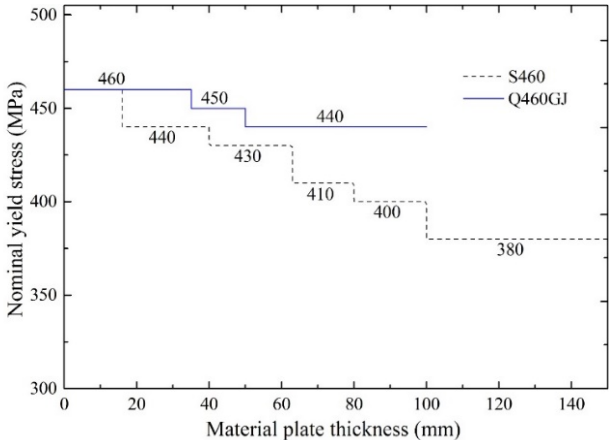

Fig. 1 Nominal yield stress variations with the material plate thickness of Q460GJ and S460 structural steel

In 20th century, there were a lot of research studies about the residual stress [2]-[4] on the Normal Strength Steel (NSS). The residual stress distributions for different shape sections, different manufacturing processes were extensively studied and the conclusions have been adopted in many national codes [5]-[7]. In recent years, some studies [8]-[14] were performed for structural members fabricated from HSS plates with 460~690 MPa yield strength. Dae-Kyung Kim et al. [11] tested two specimens fabricated by the thermos-mechanical control process without the costs of quenching, tempering, and alloying. Wang et al. [12] investigated three welded 460 MPa I-shaped sections by both sectioning method and hole drilling method. Ban et al. [13] tested seven sections of various sizes with fillet welds and one section fabricated through butt and fillet combined welds. There are only two examples in literature about heavy sections. Yang et al. [14] investigated the residual stresses on eight full scale H-sections welded by flame-cutting Q460GJ steel plates, including five doubly symmetric sections and three singly symmetric sections. Spoorenberg et al. [15] carried out an experiment program on

Qian Zhu is with the School of Civil Engineering, Chongqing University, Chongqing 400045, China, Key Laboratory of New Technology for Construction of Cities in Mountain Area (Chongqing University), Ministry of Education, Chongqing 400045, China (phone: 0089-13436186736; fax: 023-65123511; e-mail: zq-0104@outlook.com).

Shidong Nie, Bo Yang, Gang Xiong, and Guoxin Dai are with the School of Civil Engineering, Chongqing University, Chongqing 400045, China, Key Laboratory of New Technology for Construction of Cities in Mountain Area (Chongqing University), Ministry of Education, Chongqing 400045, China (e-mail: 380999766@qq.com, yang0206@cqu.edu.cn, 1957044148@qq.com, dgx1018@126.com).

two heavy quenched and self-tempered sections with section flange thickness greater than 100 mm. In HPS heavy sections, the distribution of residual stress may be quite complicated. No literature about the residual stresses on welded heavy sections fabricated from Q460GJ structural steel plates can be found. Up to now, in the welded medium-walled I-shaped sections fabricated from Q460GJ structural steel plates, the residual stress distribution is still not clear.

This paper presents the experimental investigation on the residual stresses in four welded medium-walled I-shaped sections fabricated from Q460GJ structural steel plates.

II. Experimental Program

A. Experimental Preparation

The details of four medium-walled sections (H1-H4) are listed in Table I. The geometrical symbols of these sections are shown in Fig. 2. Flame-cut steel plates with nominal thicknesses of 12 mm, 25 mm were adopted to fabricate the specimens in this study. Four medium-walled sections used fillet weld whose size is 10 mm.

TABLE I
SPECIMEN GEOMETRIC DIMENSIONS

Specimen	Dimension	H (mm)	B (mm)	t_w (mm)	t_f (mm)	b_f/t_f	h_w/t_w
H1	314x312x12x25	314	312	12	25	6	22
H2	266x262x12x25	266	262	12	25	5	18
H3	218x212x12x25	218	212	12	25	4	14
H4	170x162x12x25	170	162	12	25	3	10

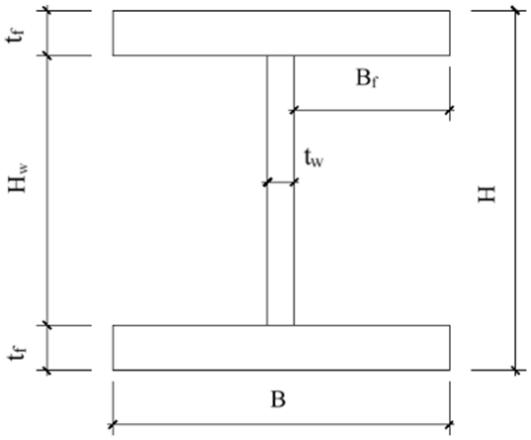

Fig. 2 Sectional dimension symbols

Tensile coupon tests on the Q460GJ structural steel plates adopted in the four specimens were carried out. A summary of the elastic modulus, yield strength, ultimate tensile stress is listed in Table II. The test results also show that the stress-strain curves of all the standard tensile coupons display an obvious yield plateau, as shown in Fig. 3. However, many researchers mentioned that there was no obvious yield plateau in the HSS, which was not observed in this study.

TABLE II
TENSILE COUPON TEST RESULTS

Thickness of steel plate t (mm)	Elastic modulus E (GPa)	Yield strength R_{eH} (MPa)	Ultimate tensile stress f_u (MPa)
12	212	571	694
25	211	482	619

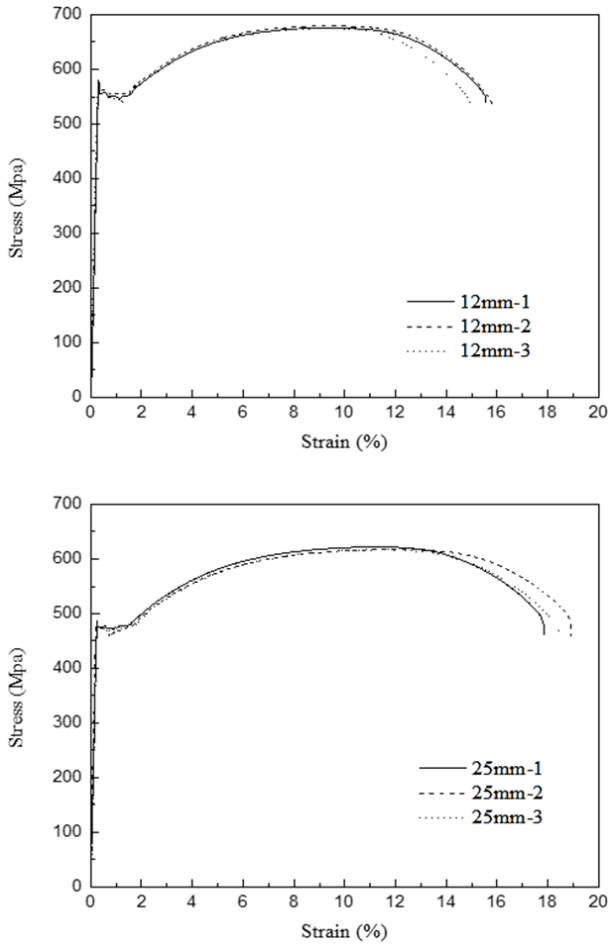

Fig. 3 Stress-strain curves of Q460GJ structural steel plates

B. Measurement Procedure

The experimental procedure followed this basic principle of sectioning method, as shown in Fig.4. Drill holes were prepared before cutting. The drilling quality of gage holes has a great

influence on the accuracy of the strip length measurement, so the drilling gage holes was conducted carefully. On the medium-walled sections, the holes with a diameter of 2 mm were drilled. All of the flanges were drilled through the whole plate thickness by through-holes, except the center of medium-walled flanges, because the through-holes with a diameter of 2 mm in this area cannot be achieved. The 12 mm thick section webs were only drilled on one side. Gage holes on the welds between flange and web were drilled normally to the surface of welds. After drilling, the initial reading of the exposed surface was measured. A reference bar made by the same material with the experimental specimens was used to eliminate the influence of temperature. A Whittemore gauge with the accuracy of 0.001 mm was employed to measure length. Due to certain strips without sufficient space for the Whittemore gauge, such as the strips on welds between flange and web, and some strips exceeding the measurement range of the Whittemore gauge, an electronic digital displaying caliper was used to replace the Whittemore gauge. Subsequently, the test sections were removed from the specimens, a distance of 1.5 times of the section height is used to eliminate end effect. And then the test sections were divided into separate plates. Furthermore, the independent plates were cut into thick strips, and finally thick strips were layered into the experimental strips. Owing to the uncertain distribution pattern of residual stress of the Q460GJ structural steel plates, cutting follows one by one, as shown in Fig. 4, which has no effect on final results, because the fibers are in the linearly elastic stage.

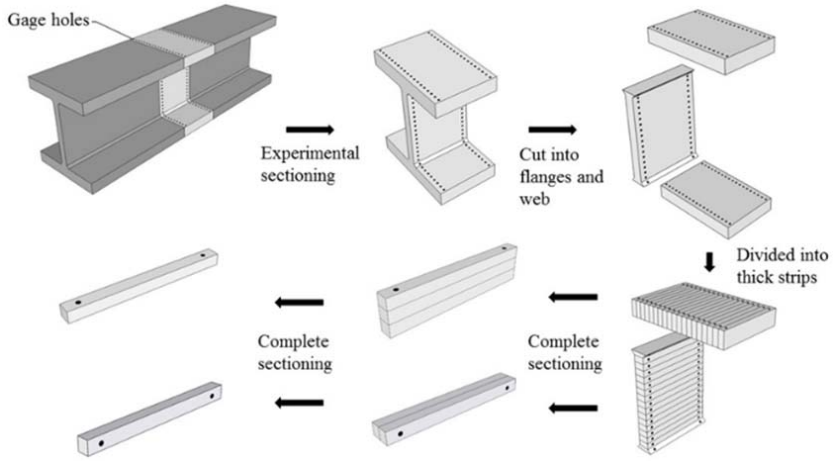

Fig. 4 Steps of sectioning method

Some strips may occur bending after the release of residual stress, especially the strips at regions with sharp stress gradients. Inhomogeneous deformation of fibers may be responsible for this phenomenon. The approach described in Sherman's paper [16] and the method proposed by Yang et al. [14] were used to correct the curved shape, in order to obtain the real length of the strips.

III. Test Results and Discussions

A. Longitudinal Residual Stresses Results

The initial measurements of both inner and outer layer were obtained before cutting, except the region at the junction between flanges and web. Therefore, the initial measurement of the inter layer were obtained by the interpolation of internal and external data. The residual stresses were obtained by the residual strains multiplied by Young's modulus. Then, circular curve correction was adopted in data analysis. Both surfaces residual stresses of strips were corrected separately and the average values were calculated as the final residual stresses. The average value is identified as more close to the truth-value. Although the results of residual stresses from straightening measurement method can be obtained from the experimental results on one side, we still access to the average values of the experimental results on both sides.

Fig. 5 shows the measured distribution and magnitude of residual stress in H1-H4 sections. As can be seen from Fig. 5, because there is no through-holes in center of medium-walled section flanges, there are no data at the inner layer of flanges near the welds. In terms of two different methods, the distribution of residual stresses is consistent, and the magnitude of residual stress agrees each other closely except for some individual points. However, the results of the two methods in outer layer near the welds show difference. The reason can be that the process of welding makes the disturbance to the surrounding. This kind of disturbance makes the irregular surface and the apparently curve of the strips. Also, the values of left and right regions around the welds in the inner surface on the flanges are obviously different, which is caused by the welding procedure. In general, the distribution of residual stresses in flanges and webs is basically symmetrical. The residual stresses from the welds to edge of flanges and the center of the web are mainly in compression, while the tensile residual stresses are displayed at the junction of web and flange and portion of the web near the junction and both ends of flanges which were influenced by flame cutting. The overall compression value of the web is lower than that of the flange. The maximum value of compressive stress occurs in the

compression zone of flanges, and at the same time the maximum value of tensile stress occurs in the junction of web and flange.

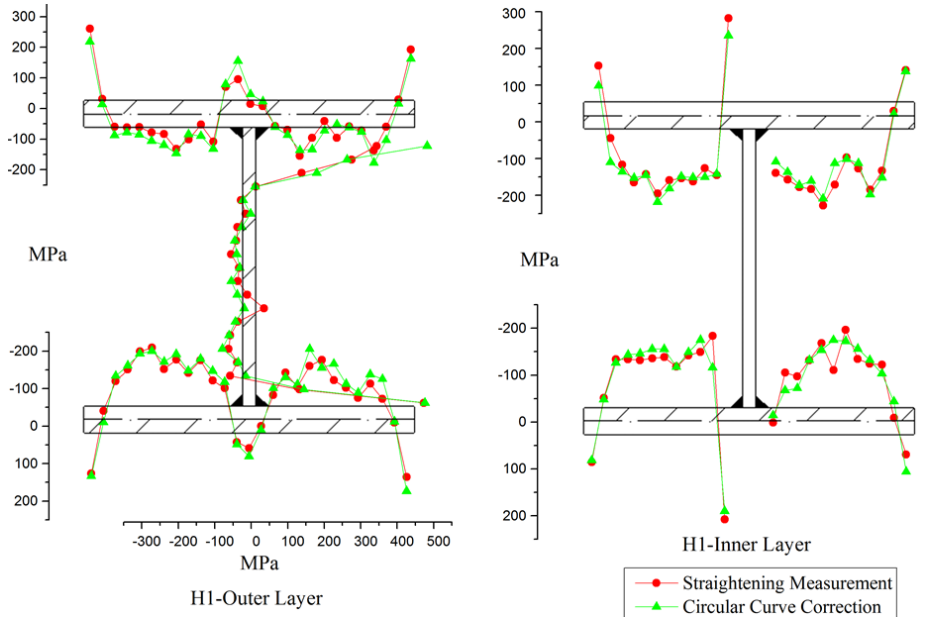

(a)

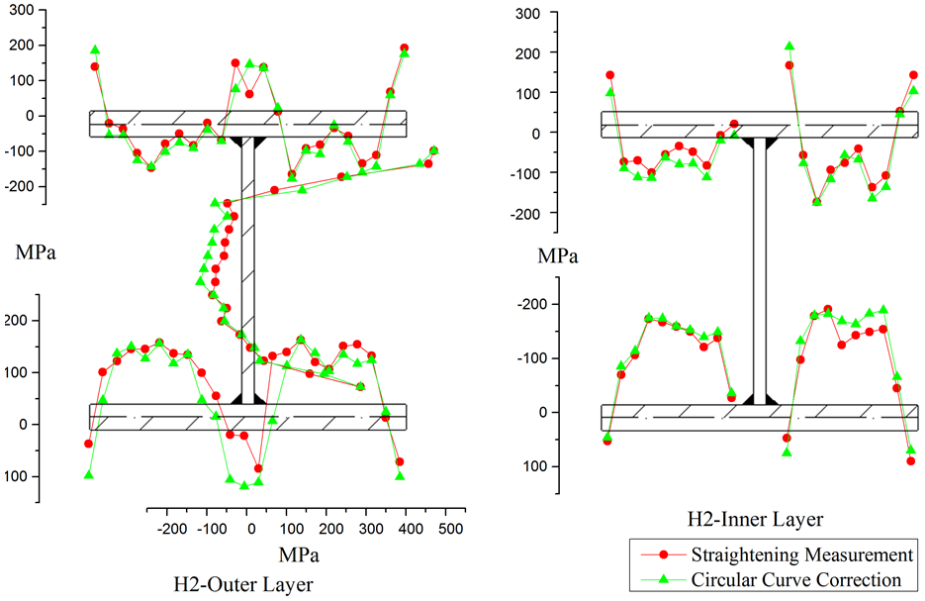

(b)

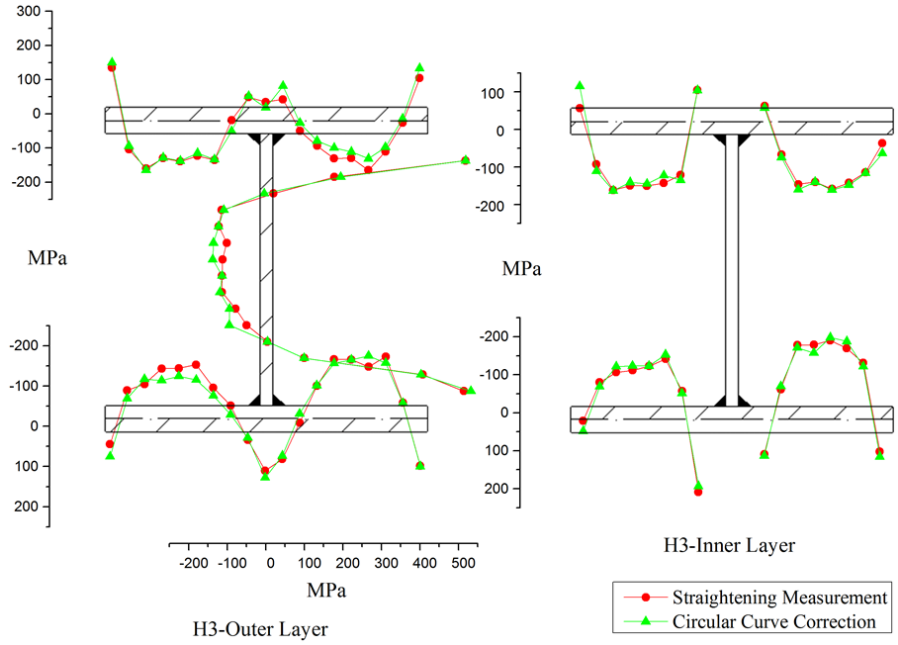

(c)

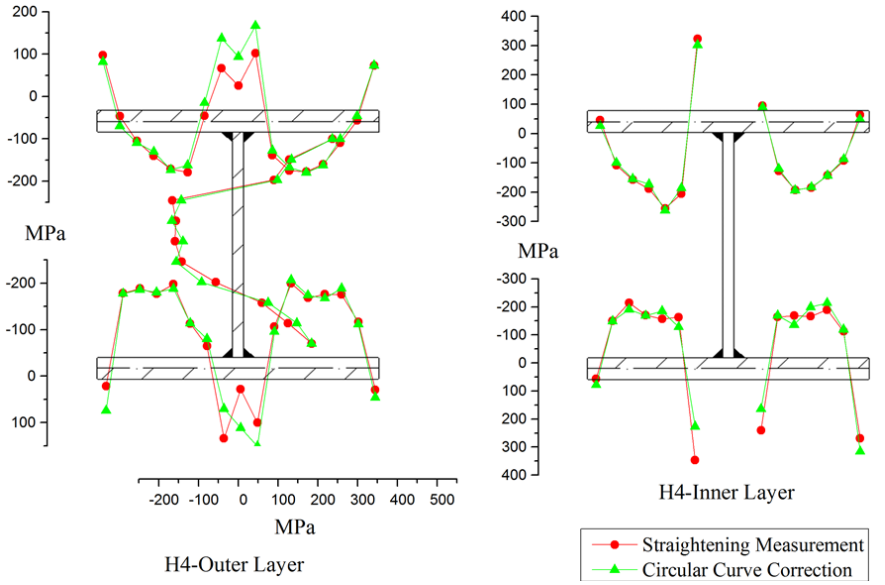

(d)

Fig. 5 Residual stress distribution in Specimens H1-H4

B. Self-Equilibrium

Without external force, residual stress serves as self-stress which should be their own balance. In the other words, self-equilibrium must be zero. Therefore, the self-equilibrium error (σ_{err}) of the whole cross-section is an assessment of the results accuracy. In this study, using the corrected residual stresses, we examined the self-equilibrium for the whole section. The self-equilibrium is defined by (1):

$$\sigma_{err} = [\sum_{i=1}^{n} A_i \cdot \sigma_{ri}]/A \quad (1)$$

where A_i is the area of a strip, A is full section area, σ_{ri} is the residual stress value at the strip location, and n represents the number of strips of the entire section. Because there are no data in the junction of flanges and webs in inlayer for medium-walled sections, the data of this location are replaced by the results at the same location of the outer layer, which may lead to tiny mistake. The summary of residual stresses self-equilibrium error obtained from different correction methods is shown in Fig. 6, which implies that almost all the closing error of the cross-sections are lower than 3% nominal

yield. Because the circular curve correction is used widely, and confirmed more. All the subsequent analyses are based on the results from curve correction method.

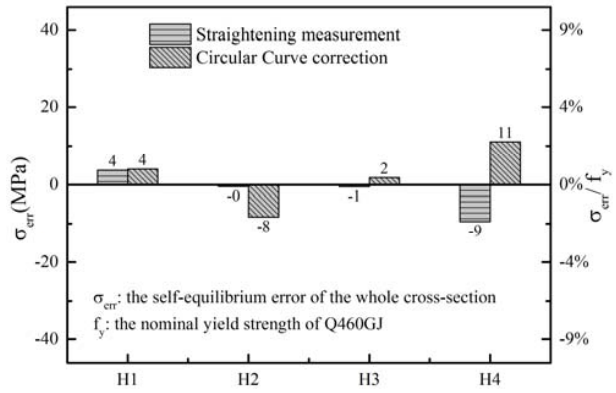

Fig. 6 Comparison of the closing error in entire cross-section from two methods

C. Interaction of Flanges and Web

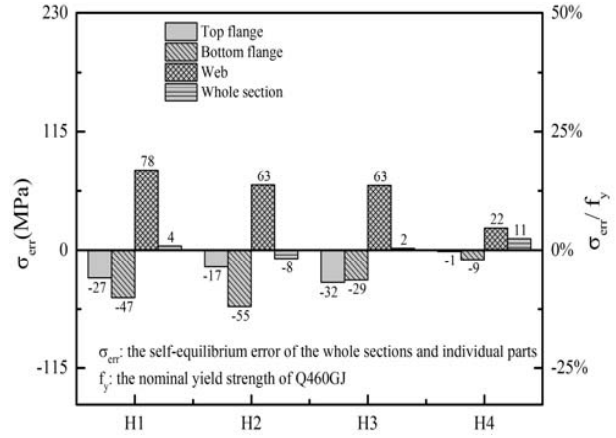

Fig. 7 Residual stress closing error of the whole sections and individual parts

The self-equilibrium errors of the individual flange and web have been calculated examined for the sake of investigating interaction of flange and web, which cannot be reflected by the self-equilibrium error of the whole cross-section. Fig. 7 displays the self-equilibrium errors of the individual flange and web of all the specimens. As it is generally accepted, there is no interaction between web and flange, and the self-equilibrium errors of individual flange and web can be ignored. However, this conclusion may not be correct for the medium-walled sections. Fig. 7 presents that the flanges are under compression, while the webs are in tension. The mutual interference between the flange and the web makes the self-equilibrium error of the whole section small. Thus, it can be concluded that the self-equilibrium in the individual flange and web may not be satisfied. The interaction between flanges and webs exists, and this should be considered in the proposed residual stress model.

IV. Residual Stress Model

Fig. 8 shows some existing models of residual stress for flame-cutting welded H sections. The model (a) in Fig. 8 was proposed based on some experimental results [17]. Li et al. [18] proposed another model, also based on experimental results, as given in Fig. 8 (b). Chinese standard [7] adopted a simplified model for structural analyses, as shown in Fig. 8 (c). The models mentioned are all based on the experimental results of NSS sections. Model (d) was introduced by Chernenko and Kennedy [19] after reviewing the former experimental data. The models mentioned above focused on NSS. Recently, some researchers studied the difference between NSS and HSS. Model (e) was proposed by Ban et al. [13] based on the experimental tests of 460 MPa welded steel H sections. Another model (f) proposed by Wang et al. [12] was also based on the investigation of 460 MPa welded steel H sections. It should be noted that the residual stress models of HSS sections ignored the interaction between flange and web, and the variation of residual stress through thickness was not taken into consideration. Models (g) and (h) proposed by Spoorenberg et al. [15] were found about the residual stresses on heavy steel sections based on experimental investigations. But Spoorenberg et al. [15] studied hot-rolled sections, of which the residual stress distributions may be quite different from flame-cutting welded sections.

Though ECCS [20] put forward that the residual stresses on thick-walled sections have an obvious thickness effects, which significantly influence the ultimate strength of columns, there was no specified model in ECCS. In addition, the residual stresses in the individual web or flange are not in self-equilibrium. This phenomenon and all the mentioned factors will be considered in the proposed residual stress model for welded medium-walled sections.

All the experimental data of residual stress in medium-walled sections have been fitted as the segment lines by MATLAB [21]. The segment line fitting of the experimental results was conducted by the least square method, and then considering the interaction between flanges and web and the whole section self-equilibrium assumption, the fitted segment lines were adjusted accordingly. The obtained data of every section are compared to the fitted segment lines for medium -walled sections in Fig. 9, which displays that the fitted segment lines were in good agreement with the experimental data. It is prominent that the fitted lines are different between layers of flanges. A multilayer residual stress model is proposed for considering these characteristics. The proposed model is shown in Fig. 10 with five residual stress values at specific locations, which are the residual stress values at flange edge (σ_{fre}), at the compressive region of flange (σ_{frc}), at the middle of the flange (σ_{frt}), at the two ends of web (σ_{wrt}), and at the middle of web (σ_{wrc}). The suggested values are based on the average of the fitting results of every section, which are listed in Table III. In this table, σ represents the ratio of residual stress to yield stress (R_{eH}), a, b, c, and d on flange represent the ratios of location on flange to the flange width (B), and e and f on web represent the ratios of location on web to the web height

(H_w). It should be noted that the recommended residual stress model is proposed for 460 MPa welded medium-walled I-shaped sections.

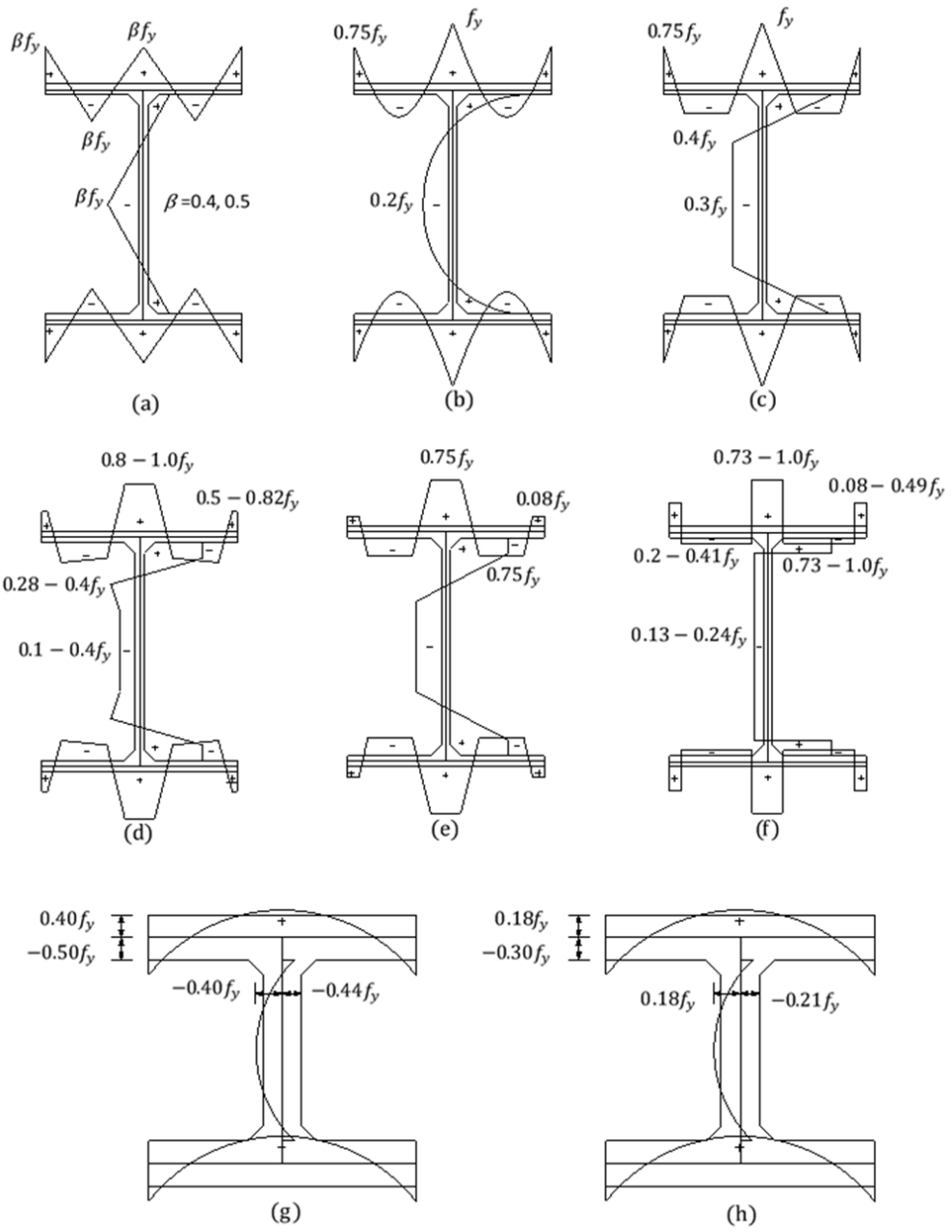

Fig. 8 Existing models of the residual stress for flame-cutting welded H sections

TABLE III
SUGGESTED VALUES OF RESIDUAL STRESS MODEL

Locations	Suggested value										
	σ_{fre}	σ_{frc}	σ_{frt}	σ_{wrt}	σ_{wrc}	a	b	c	d	e	f
outside flange	0.27	-0.24	0.25	-	-	0.05	0.08	0.24	0.08	-	-
inside flange	0.19	-0.28	0.31	-	-	0.05	0.07	0.23	0.08	-	-
web	-	-	-	0.74	-0.14	-	-	-	-	0.09	0.17

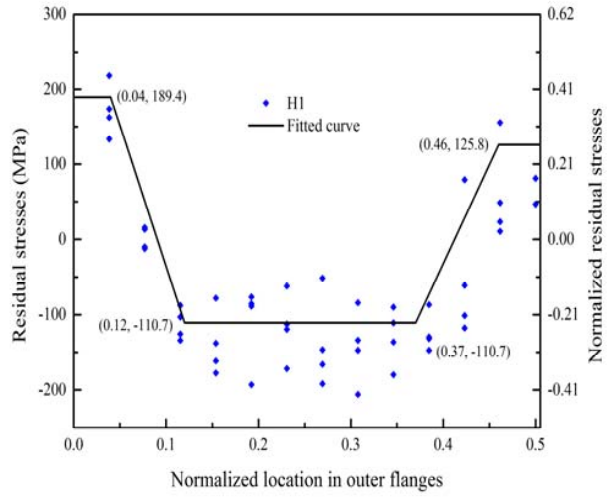
H1
Fitted curve
(0.04, 189.4)
(0.46, 125.8)
(0.12, -110.7)
(0.37, -110.7)
Residual stresses (MPa)
Normalized residual stresses
Normalized location in outer flanges

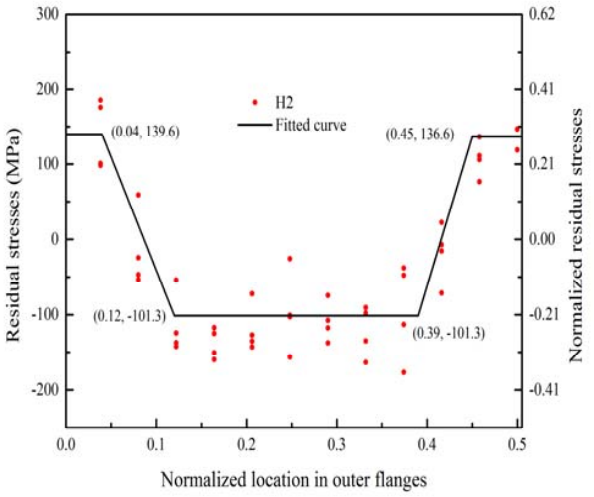
H2
Fitted curve
(0.04, 139.6)
(0.45, 136.6)
(0.12, -101.3)
(0.39, -101.3)
Residual stresses (MPa)
Normalized residual stresses
Normalized location in outer flanges

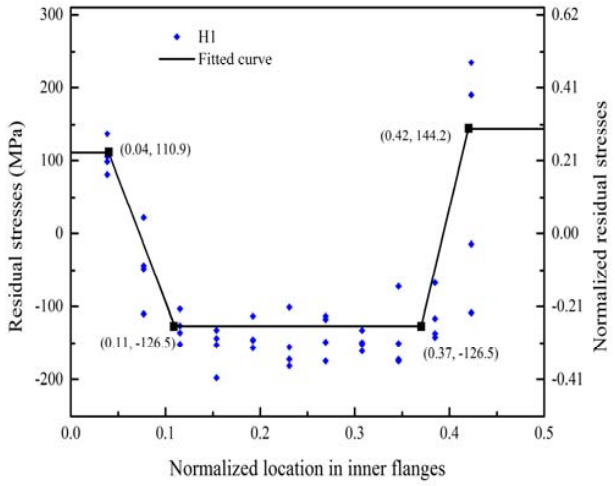
H1
Fitted curve
(0.04, 110.9)
(0.42, 144.2)
(0.11, -126.5)
(0.37, -126.5)
Residual stresses (MPa)
Normalized residual stresses
Normalized location in inner flanges

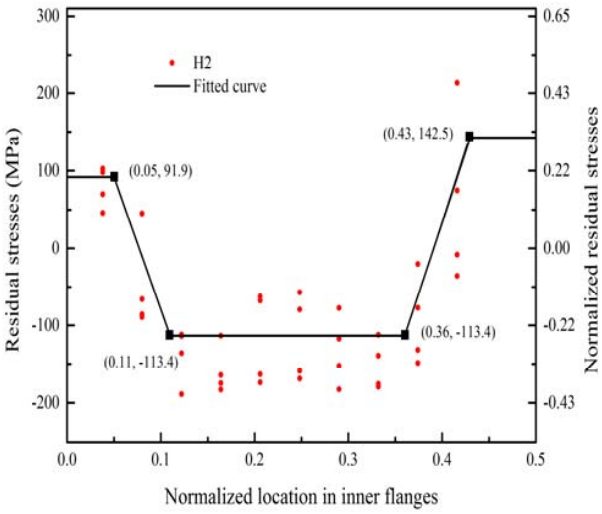
H2
Fitted curve
(0.05, 91.9)
(0.43, 142.5)
(0.11, -113.4)
(0.36, -113.4)
Residual stresses (MPa)
Normalized residual stresses
Normalized location in inner flanges

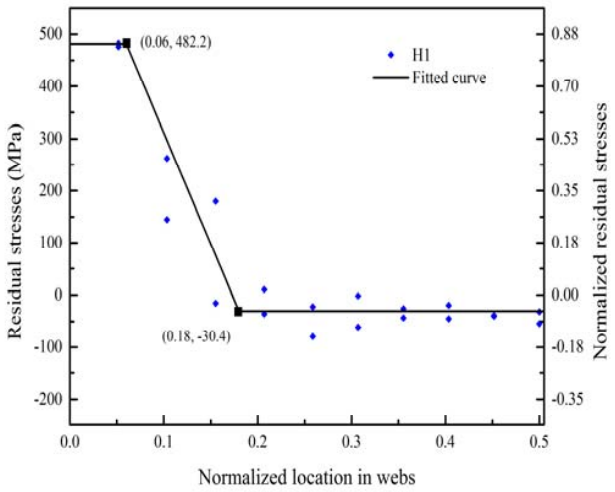
H1
Fitted curve
(0.06, 482.2)
(0.18, -30.4)
Residual stresses (MPa)
Normalized residual stresses
Normalized location in webs

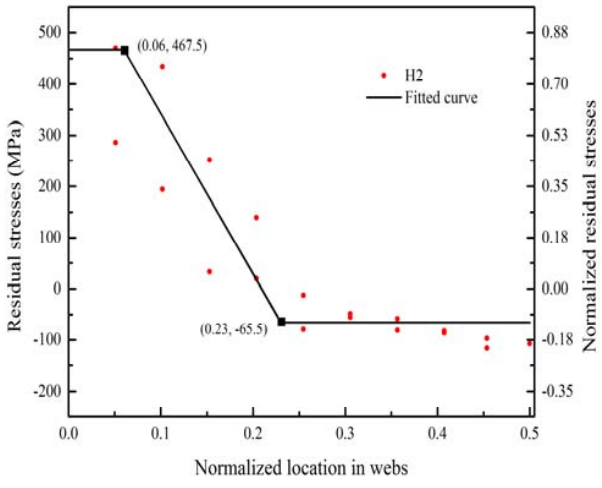
H2
Fitted curve
(0.06, 467.5)
(0.23, -65.5)
Residual stresses (MPa)
Normalized residual stresses
Normalized location in webs

(a) (b)

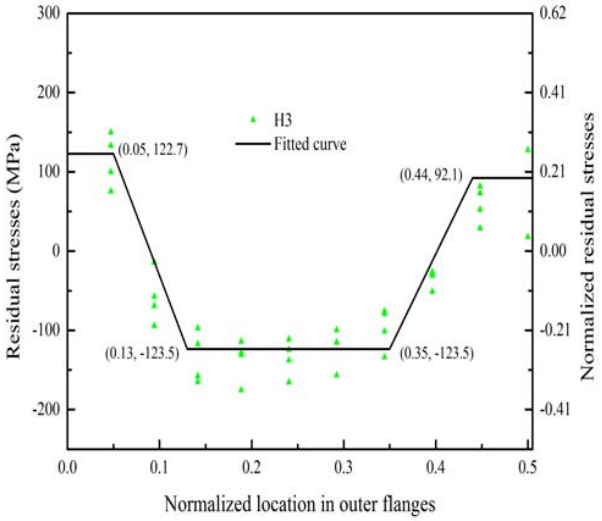

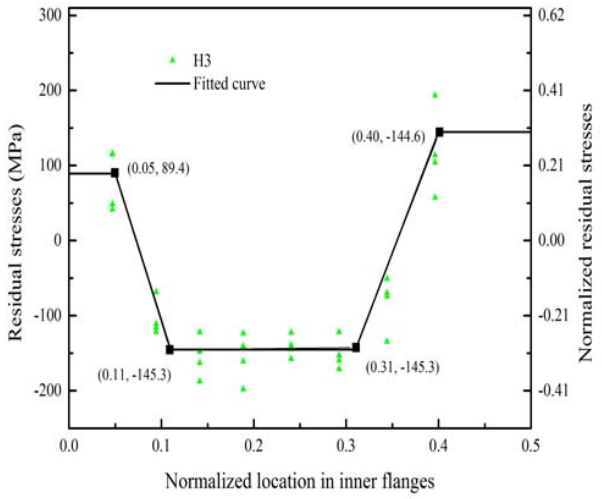

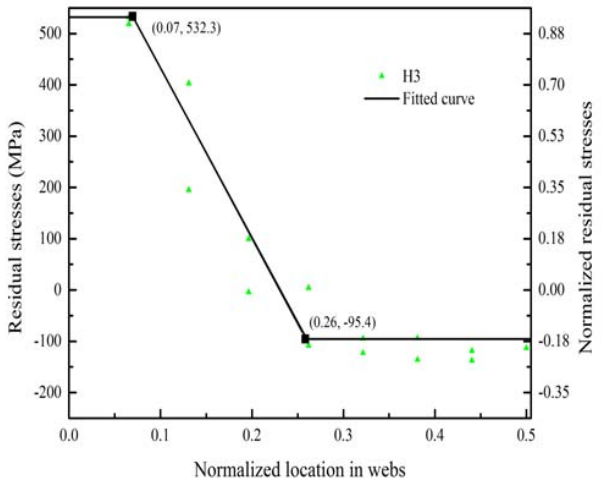

(c)

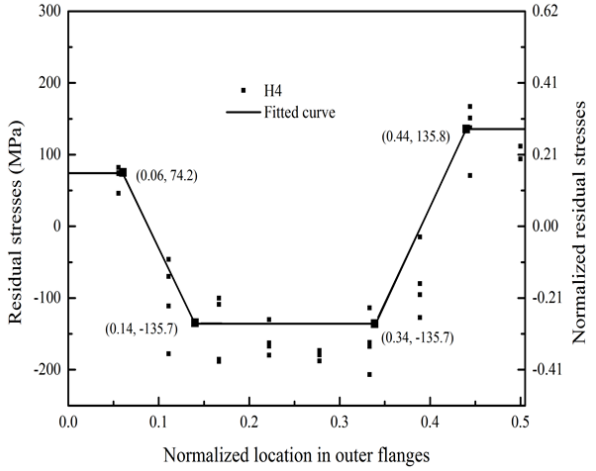

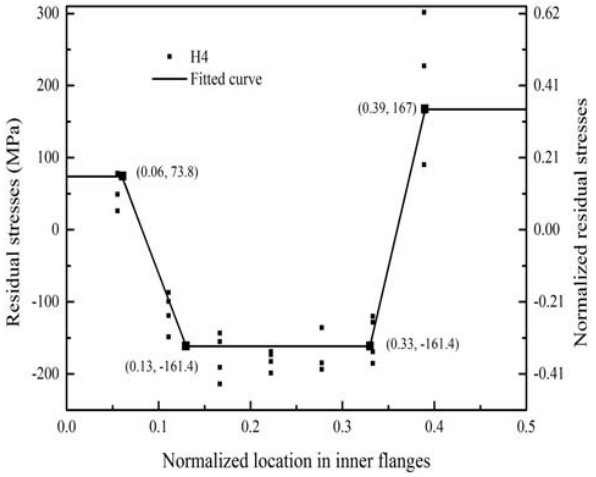

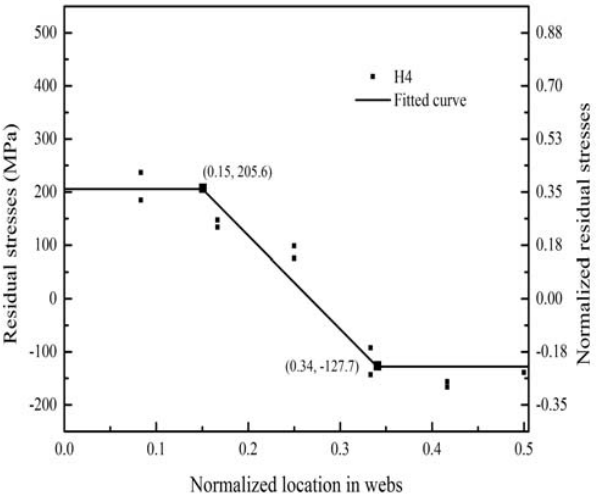

(d)

Fig. 9 Residual stress data of Specimens H1-H4. Note: Normalized location is the ratio of actual location to the width, Normalized residual stresses is the ratio of test residual stresses to yield stress

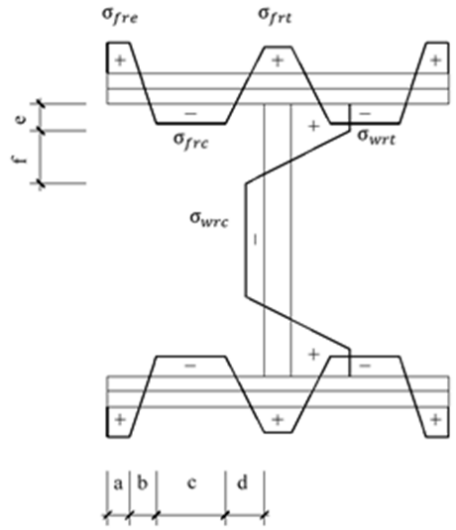

Fig. 10 Proposed residual stress model

Compared to the typical residual stress model which represents the model ignored the interaction between flange and web, and the variation of residual stress through thickness, this multilayer model accurately reflects the characteristics of medium-walled section. Using the typical existing residual stress models, it may not be conservative to analyze the load-carrying capacities of the columns with medium-walled sections. The proposed multilayer residual stress model can reflect the residual stress variation through thickness, and this model is more appropriate for structural analyses on medium-walled section members.

V. Conclusions

This study investigates the magnitude and distribution of residual stresses on welded I-shaped medium-walled sections fabricated from Q460GJ flame-cutting plates. As a result, the following conclusions can be drawn:

(1) The experimental results indicate that the flange edges, the middle of flanges and the junction of web and flange were under tension, while compressive residual stresses were found in other regions of the sections.
(2) With the increase of the distance from the welds to the out surface of the flange, the influence of the welding is significantly reduced.
(3) The residual stress self-equilibrium in the individual flange and web may not be satisfied in medium-walled. Therefore, the interaction between flanges and web exists, and which should not be ignored when proposed residual stress model.
(4) A multilayer residual stress model is proposed for 460 MPa welded medium-walled I-shaped sections in this study. The proposed multilayer residual stress model has a great agreement of experimental results.

Acknowledgment

The authors gratefully acknowledge the sponsorship from the National Natural Science Foundation of China (No. 51578089 and No.51078368) and the Fundamental Research Funds for the Central Universities (No. CDJZR12200007 and No. CDJZR12200005).

References

[1] Shi YJ. Development and application of high strength and high performance steel in buildings. Proceedings of the 3rd International Forum on Advances in Structural Engineering. Beijing: China Architecture & Building Press; 2009.p.397-407(in Chinese).
[2] Alpsten GA, Tall L. Residual stresses in heavy welded shapes. Welding Research Supplement; 1970:93-105.
[3] Fukumoto Y, Itoh Y. Statistical study of experiments on welded beams. J Struct Div1981; 107:89 – 103
[4] Wang GZ, Zhao WW. Residual stress measurement for welded and hot-rolled I section steels. Industrial Construction 1986; 16(7):32-37(in Chinese).
[5] BS EN 1993-1-1 (2005). Eurocode 3: Design of steel structures. BSI, London.
[6] ANSI/AISC 360-10(2010). Specification for structural steel buildings. AISC, Chicago.
[7] GB50017-2003. Code for design of steel structures. Beijing: China Planning Press; 2003 (in Chinese).
[8] Rasmussen K J R, Hancock G J. Plate slenderness limits for high strength steel sections. Journal of Constructional Steel Research 1992; 23(1):73-96.
[9] Rasmussen K J R, Hancock G J. Tests of high strength steel columns. Journal of Constructional Steel Research 1995; 34(1): 27-52.
[10] Beg D, Hladnik L. Slenderness limit of Class 3 I cross-sections made of high strength steel. J Constr Steel Res 1996;38:201-17.
[11] Dae-Kyung Kim, Cheol-Ho Lee, et al. Strength and residual stress evaluation of stub columns fabricated from 800Mpa high-strength steel. Journal of Constructional Steel Research; 2014; 102:111-120.
[12] Wang YB, Li GQ, Chen S. Residual stresses in welded flame-cut high strength steel H-sections. Journal of Constructional Steel Research 2012; 79:159-165.
[13] Ban HY, Shi G, Bai Y, et al. Residual stress of 460 MPa high strength steel welded I section: experimental investigation and modeling. International Journal of Steel Structures 2013; 13(4): 691-705.
[14] Bo Yang, Shidong Nie, et al. Residual stresses in welded I-shaped sections fabricated from Q460GJ structural steel plates. Journal of Constructional Steel Research; 2016;122:261-273.
[15] R. C. Spoorenberg, H. H. Snijder, et al. Experimental investigation on residual stresses in heavy wide flange QST steel sections. Journal of Constructional Steel Research; 2013;89:63-74.
[16] Sherman DR. Residual stress measurement in tubular members. Structural Division Proceedings of the American society of Civil Engineers 1969(4):635-647.
[17] Chen Ji. The stability coefficient of axially loaded compression members for summarizing the effect of residual stress, eccentricity and initial out-of-straightness. China Technical Committee for Standards of Steel Structures, Beijing; 1982:1-14(in Chinese)
[18] Li KX, Xiao YW, et al. Column curves for steel compression member. Journal of Chongqing Institute of Architecture and Engineering 1985:24-33 (in Chinese).
[19] Chernenko DE, Kennedy DJL. An analysis of the performance of welded wide flange columns. Canadian Journal of Civil Engineering; 1991.
[20] ECCS. Manual on stability of steel structures. Part 2.2 Mechanical Properties and Residual Stresses. ECCS Publ.: 1976.
[21] Saeed Moaveni. Engineering Fundamentals: An Introduction to Engineering. Minnesota State University. Thomson Engineering; 2015.